Materials Science Forum
ISSN: 1662-9752, Vol. 1062, pp 204-208
doi:10.4028/p-98r1yh
© 2022 The Author(s). Published by Trans Tech Publications Ltd, Switzerland.
Submitted: 2021-10-15
Revised: 2022-03-16
Accepted: 2022-03-16
Online: 2022-05-31

Graphite Assisted P and Al Implanted 4H-SiC Laser Annealing

Cristiano Calabretta[1,a*], Alessandro Pecora,[2,b],
Marta Agati[1,c], Stefania Privitera[1,d], Annamaria Muoio[1,e],
Simona Boninelli[1,f] and Francesco La Via[3,g]

[1]CNR-IMM, VIII Strada, 5, 95121
Catania, Italy

[2]CNR-IMM, Via del Fosso del Cavaliere,
100 - 00133 Roma, Italy

[a]cristiano.calabretta@imm.cnr.it, [b]alessandro.pecora@cnr.it, [c]marta.agati@imec.be,
[d]stefania.privitera@imm.cnr.it, [e]annamaria.muoio@imm.cnr.it, [f]simona.boninelli@imm.cnr.it,
[g]francesco.lavia@imm.cnr.it

Keywords: 4H-SiC; Laser Annealing; XeCl; dopant activation; phosphorus; aluminum; defects; TEM; Raman; SEM;

Abstract. This paper discusses a novel annealing technique for 4H-SiC implants which involves the use of pulsed XeCl laser (λ=308 nm). In particular, an absorbing graphitic coating is used to protect the sample from surface atoms desorption or phase separation. Both conventional furnace annealing and laser annealing on P and Al implants, commonly employed for source and body in metal-oxide-semiconductor field-effect transistors (MOSFETs), were examined through Transmission Electron Microscopy (TEM), μ–Raman spectroscopy and Scanning Electron Microscopy (SEM). It is shown that the implant activated through traditional thermal annealing at 1650 °C for 30 min has a large network of dislocation loops, while they do not appear to be present in the laser annealed implant. Through Raman spectroscopy and SEM investigations both the crystalline quality of the laser annealed sample and the integrity of the surface were attested.

Introduction

As a result of new developments in SiC crystal growth and process technologies, the manufacturing of power MOSFETs has begun. Source and body regions in MOSFETs are achieved by ion implantation and subsequent mandatory thermal annealing at T > 1600 °C [1]. However, in this temperature regime generation of C interstitial-vacancies couples is registered along the whole epitaxial layer, affecting carrier mobility and lifetime in channel region. Particularly, carbon vacancies have been found to be the origin of the so called $Z_{1/2}$ and EH_7 deep energy levels: the main carrier lifetime killers in 4H-SiC [2]. In addition, a network of dislocation loops is also produced in the implant projected range together with not satisfactory activation rates [3-4]. To work around these issues, pulsed-laser-based methods have been applied for post-implant annealing of P and Al doped 4H-SiC epitaxial layers in order to recover the crystal structure and to electrically activate the doping species. Although this technique has proven effective activation results, it has not yet reached maturity as industrial process, due to the scarce control over the surface damage caused by laser radiation-SiC interaction. Unlike silicon, 4H-SiC does not favor post-melting epitaxial regrowth [5-6-7]. This work, therefore, shows a pioneering method to acquire a substantial control over irradiated surface quality, allowing to implement implanted 4H-SiC crystalline and electrical properties.

This article is an open access article under the terms and conditions of the Creative Commons Attribution (CC BY) license
(https://creativecommons.org/licenses/by/4.0)

Materials and Methods

The experiments were carried out on a Cree-supplied SiC wafer with a nitrogen concentration of 10^{18} N/cm^3. Then, a 6 µm epitaxial layer was grown along the (0001) 4° off-axis direction through low pressure hot wall chemical vapor deposition. Source P ion implantation was performed at 500 °C with energies varying from 30 to 200 keV and fluences ranging from 10^{13} to 10^{14} cm^{-2} in order to generate an almost uniform doped layer ~220 nm thick with a concentration of 10^{20} cm^{-3}, while body Al implant was characterized by 10^{17}Al/cm^3 550 nm thick implanted layer [8]. Photoresist was spin coated on sample surfaces and pyrolyzed at ~ 1000 °C in order to achieve graphitization on surface. Final 90 and 180 nm thick layers were deposited on double P and Al implanted SiC samples. Once irradiated by means of a XeCl laser source (λ =308 nm) with 40 Hz pulse and 1000 shots/point, graphite was removed through oxygen plasma attack. For comparison, some samples were left uncoated and another underwent heat treatment at 1650 °C for 30 min. Experimental investigation was carried out by means of TEM and SEM microscopy, and micro-Raman spectroscopy through He-Cd (λ=325 nm) laser source.

Discussion

The technique exploits irradiations over a graphitic absorber layer. Indeed, thanks to its 3800 °C melting temperature and high absorption coefficient, graphite is the best candidate to fully absorb laser radiation, allowing a heat diffusive regime along the underlying implanted 4H-SiC. Fig. 1 displays the XTEM acquisition from two samples subjected to furnace annealing and graphite assisted laser annealing at 0.6 J/cm^2.

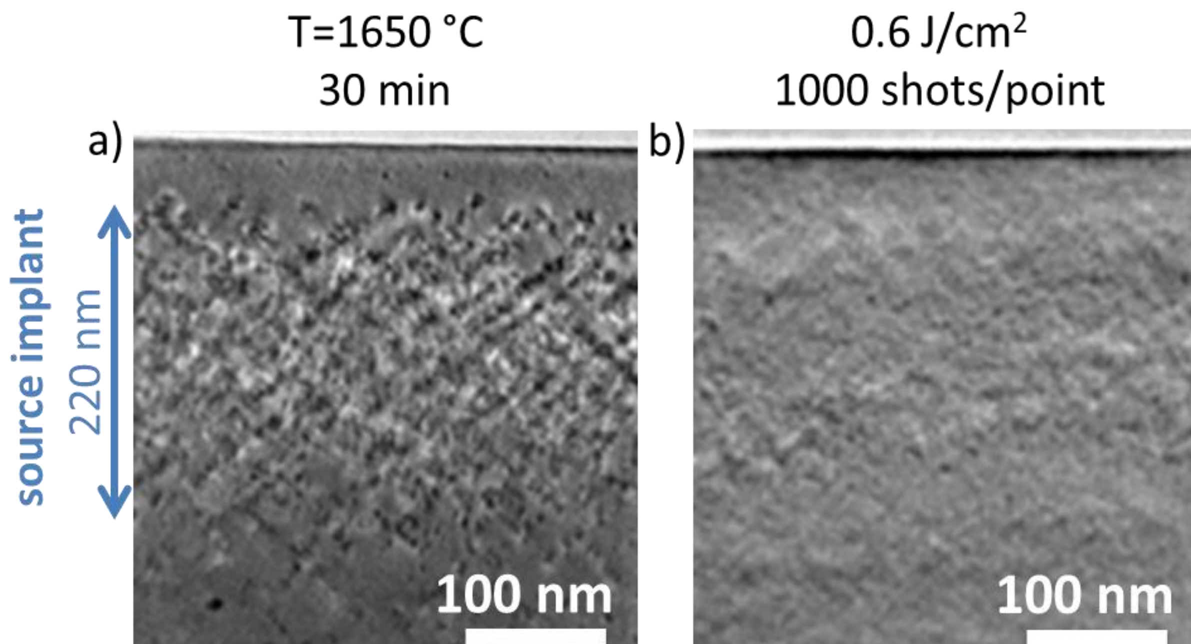

Figure 1. XTEM images of two samples processed with conventional thermal annealing at T=1650 °C for 30 min and laser annealing at 0.6 J/cm^2 1000 shots/point.

In Fig. 1a the sample processed at 1650 °C for 30' shows dense dislocation loops network related to the 250 nm thick source region as a consequence of point defects aggregation stimulated by high temperature annealing, under thermal equilibrium conditions. The 550 nm thick body region, below the source implant, is affected by rear aggregates and follows the lower Al implant concentration. Indeed, owing to the lower implanted dose, the amount of interstitials available for the generation of extra-planes is consequently lower in body region. In Fig. 1b laser annealed sample presents limited source region defectiveness and the body region is remarkably free from dislocation loops. It can be deduced that, if on the one hand the shorter diffusion times result in a smaller dislocation loops size distribution, on the other hand it is known that thermal non-equilibrium regime is effective in preventing generation of point defects. Micro-Raman spectroscopy attested SiC characteristic Raman modes restoration, as indication of the effective crystalline recovery following laser treatment. In particular, Fig. 2a exhibits how lattice subjected to laser annealing is sensible to the applied laser energy density. The analyses were performed through a He-Cd laser source (λ=325 nm) on the samples after graphite remotion by oxygen plasma etching. The UV laser was required to investigate the two implanted layers and minimize the signal from underlying substrate and epitaxial layer. Following a statistic on the average spectrum extracted from μ-Raman maps under backscattering conditions, the polynomial fits with 68 % confidence bands of transverse optic E_2(TO) full width at half maximum (FWHM) are displayed. From comparison it emerges that FWHM shows improving trend with graphitic layer thickness. When irradiated under 180 nm graphitic layer, SiC exhibits E_2(TO) FWHM ~4.5 cm^{-1}, slightly lower than in furnace annealed SiC, thus corroborating TEM analysis. Samples subjected to laser annealing with uncoated surface exhibit FWHM decreasing with energy up to 0.6 J/cm^2 threshold. However, such behavior could be attributed to implant etching and SiC oxidation phenomena exposing the underlying SiC epitaxy. Above 0.60 J/cm^2, the progressive increase in FWHM testifies how SiC is affected by melting processes which determine crystalline deterioration.

The covering effect of the graphite layer on SiC is displayed in SEM micrographs taken on uncoated as well as 180 nm graphite coated samples and underwent laser annealing at the energy density of 0.6 J/cm^2. Indeed, to support the reported Raman results, Fig. 2b depicts how high temperatures stimulate the mobility of surface atoms, triggering their desorption and promoting consequent surface degradation. Furthermore, the spherical agregates discussed above are shown and were detected with an average size of 131 nm and with 21% of surface coverage. Such spheres detected on the surface have been identified as SiO_2 spheres through Electron Energy Loss Spectroscopy (EELS) analysis and are the consequence of surface active oxidation with the oxygen present in the chamber [9]. Figure 2c, shows the 180 nm graphite covered implant surface once the residual graphite has been removed from the sample by oxygen plasma etching. It turns out how the sample was rather preserved than the previous by the overlap of graphitic coating. These pictures demonstrate the efficacy of the coating media in preserving SiC surface during laser shots.

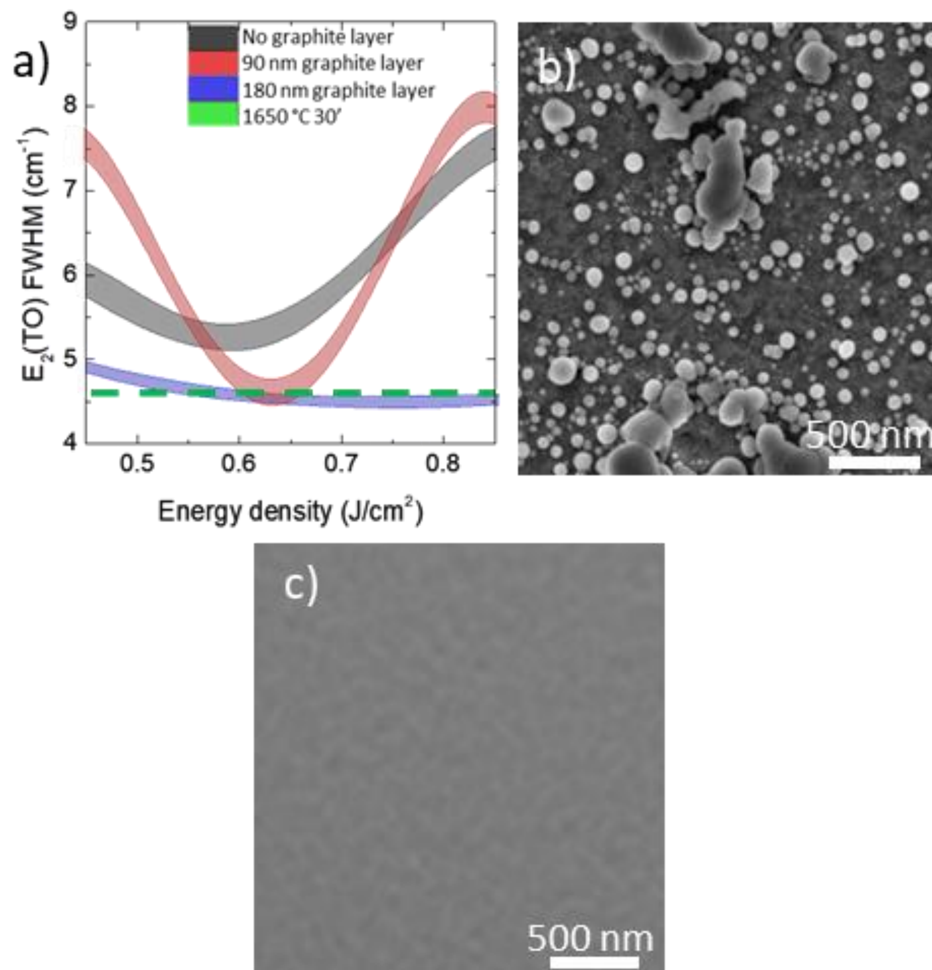

Figure 2. a) FWHM trend of E_2(TO) mode with respect to energy density for different coating thicknesses. SEM micrographs acquired on sample surface underwent 0.6 J/cm^2 laser annealing b) with no coating and c) with 180 nm coating.

Acknowledgements

This work has been supported by the European ECSEL JU project REACTION (grant agreement n. 783158).

Summary

The findings inherent to the development of an innovative laser annealing approach in order to avoid damage of the implant surface were disclosed in this study. The deposition of a graphitic coating layer is used in this approach. MOSFET's source and body implants were exposed to varying XeCl pulsed laser intensities and graphitic coating thicknesses. It was observed that using a graphite thickness of 180 nm protects the implant from surface erosion at 0.60 J/cm^2 while also demonstrating superior crystalline quality in terms of the FWHM of the Raman E_2 (TO) mode with respect to conventional furnace annealed implant. TEM analysis demonstrated the absence of extended defects within the 4H-SiC implanted area.

References

[1] A. Severino, et al. Effects of Thermal Annealing Processes in Phosphorous Implanted 4H-SiC Layers Mat.Sci Forum, 407, 2019, 963.

[2] R. Nipoti, et al. Defects related to electrical doping of 4H-SiC by ion implantation. Mater. Sci. Semicon. Proc. 78, 2017, 13–21.

[3] C. Calabretta, Thermal annealing of high dose p implantation in 4H-SiC, Mater Sci Forum, 963, 2019, 399–402.

[4] V. Šimonka, et al. Transient model for electrical activation of aluminium and phosphorus-implanted silicon carbide. J. Appl. Phys.123, 2018, 325701.

[5] Boutopoulos et al. Laser annealing of Al implanted silicon carbide: Structural and optical characterization. Appl. Surf. Sci. 2007, 253, 7912–7916.

[6] F. Mazzamuto et al. Silicon Carbide recrystallization mechanism by non-equilibrium melting laser anneal. Mater. Sci. Forum 2016, 858, 540–543.

[7] C. Calabretta et al. 4H-SiC MOSFET source and body laser annealing process, Mater Sci Forum,1004, 2020, 705–711.

[8] P. Fiorenza et al. High-Resolution Two-Dimensional Imaging of the 4H-SiC MOSFET Channel by Scanning Capacitance Microscopy, Nanomaterials 11, 2021, 1626.

[9] C. Calabretta, et al. Laser Annealing of P and Al implanted 4H-SiC epitaxial layers, Materials, 12(20), 2019, 3362.